Significant defluorination of polychlorofluorocarboxylic acids triggered by anaerobic microbial hydrolytic dechlorination

Bosen Jin[1], Huaqing Liu[1], Shun Che[1,2], Jinyu Gao[1], Yaochun Yu[1,2], Jinyong Liu[1], Yujie Men[1,2,*]

[1]Department of Chemical and Environmental Engineering, University of California, Riverside, California, 92521, United States

[2]Department of Civil and Environmental Engineering, University of Illinois at Urbana-Champaign, Urbana, Illinois, 61801, United States

***Corresponding Author**

Yujie Men

Department of Chemical and Environmental Engineering

University of California, Riverside

Address: A235 Bourns Hall, 3401 Watkins Drive, Riverside, CA 92521

Email: ymen@engr.ucr.edu; menyjam@gmail.com

Phone: (951) 827-1019

Abstract

Chlorinated polyfluorocarboxylic acids (Cl-PFCAs) derived from the widely used chlorotrifluoroethylene (CTFE) polymers and oligomers may enter and influence the aquatic environment. Here, we report significant defluorination of Cl-PFCAs by an anaerobic microbial community via novel pathways triggered by anaerobic microbial dechlorination. Cl-PFCAs first underwent microbial reductive, hydrolytic, and eliminative dechlorination, and it was the hydrolytic dechlorination that led to significant spontaneous defluorination. Hydrolytic dechlorination was favored with increased Cl-substitutions. An isolated, highly enriched anaerobic defluorinating culture was dominated by two genomes closest to *Desulfovibrio aminophilus* and *Sporomusa sphaeroides*, both of which exhibited active defluorination of CTFE tetramer acid. It implies the critical role played by anaerobic non-respiratory hydrolytic dechlorination in the fate of chlorinated polyfluoro-chemicals in natural and engineered water environments. The greatly enhanced biodegradability by Cl-substitutions also sheds light on the design of cost-effective treatment biotechnologies, as well as alternative PFAS that are readily biodegradable and less toxic.

Main

Polychlorofluoro- chemicals represent a large group of per- and poly-fluoroalkyl substances (PFAS), which have been widely applied in commercial goods and industrial materials[1-5]. The well-known ones include fluoropolymers, such as polychlorotrifluoroethylene (PCTFE)[3,6], and CTFE oligomers contained in the nonflammable hydraulic fluid[7,8]. The thermolysis of PCTFE and metabolism of CTFE oligomers by higher organisms can generate CTFE oligomer carboxylic acids[9-13]. They may enter into the hydrosphere together with other chlorinated PFAS (Cl-PFAS)[14] and ultra-short-chain chlorofluorocarboxylic acids used as building blocks for PFAS synthesis[15] or derived from chlorofluorocarbons (CFCs)[16,17], causing adverse impacts on the ecosystem. Compared to the strong C–F bonds, which rendered the sluggish microbial cleavage in a limited number of PFAS structures[18-21], C–Cl bonds have lower bond dissociation energy (BDE) and are more readily microbially cleaved[22]. Thus, the C–Cl bonds in Cl-PFAS could become vulnerable positions for microbes to attack, thus enhancing biodegradability and even the defluorination activity.

Despite the increasing detection of Cl-PFAS in diverse natural and engineered environments, including surface runoff, lakes, sediments, and wastewater treatment plants[23-28], their biodegradability and environmental fate have not yet been well documented. Studies on the transformation of Cl-PFAS by microbes and higher organisms were limited to certain structures, and reductive dechlorination was the major reported biotransformation pathway[29-31]. Whether and how environmental microbes defluorinate other important Cl-PFAS, such as CTFE oligomer acids, and how the number and position of Cl-substitutions would affect biodegradability is yet unknown.

Here, we report enhanced anaerobic biotransformation activities of a comprehensive set of environmentally important Cl-PFAS (**Table S1 & 2**) caused by three types of anaerobic microbial dechlorination of the C–Cl bonds. We demonstrated that the hydrolytic dechlorination further triggered significant defluorination of CTFE tri- and tetramer acids by elucidating the biotransformation and biodefluorination pathways. We further interpreted the structure-biodegradability relationship and identified the responsible microorganisms. The findings bring new insights into the environmental fate of Cl-PFAS, particularly the CTFE oligomer acids, PFAS source-tracking, the design of readily biodegradable alternative PFAS, and the development of cost-effective biotechnologies for the cleanup of PFAS from impacted environments.

Results

Dechlorination-induced defluorination of CTFE oligomer acids

All three CTFE oligomer carboxylic acids (i.e., **CTFE2**, **CTFE3**, and **CTFE4**) investigated in this study were completely biotransformed with significant fluoride release by the sludge community in the anaerobic condition. From the dimer to tetramer acid, with more Cl-substitutions in the structure, the half-life decreased from 19 to 3 days (**Table S3**), and the defluorination degree significantly increased from <10% to ~80% after 84 days (**Figure 1a**). Transformation product (TP) analysis indicates that the three CTFE oligomer acids all first underwent microbial dechlorination reactions, including reductive, hydrolytic, and eliminative dechlorination. Among them, hydrolytic dechlorination was the one that triggered substantial defluorination (**Figure 1b**), which became more favorable for the trimer and tetramer acids that possess more Cl-substitutions, leading to the deeper defluorination. Reductive dechlorination formed transformation products that were more recalcitrant to biotransformation and did not

contribute to the defluorination. Eliminative dechlorination led to the formation of unsaturated TPs, some of which underwent much slower reductive defluorination or hydrogenation as reported previously[19], contributing to 0 – 2 F^- release. The stable unsaturated TPs with multiple C=C bonds could also contribute to the dark yellow color developed during the defluorination of **CTFE4**.

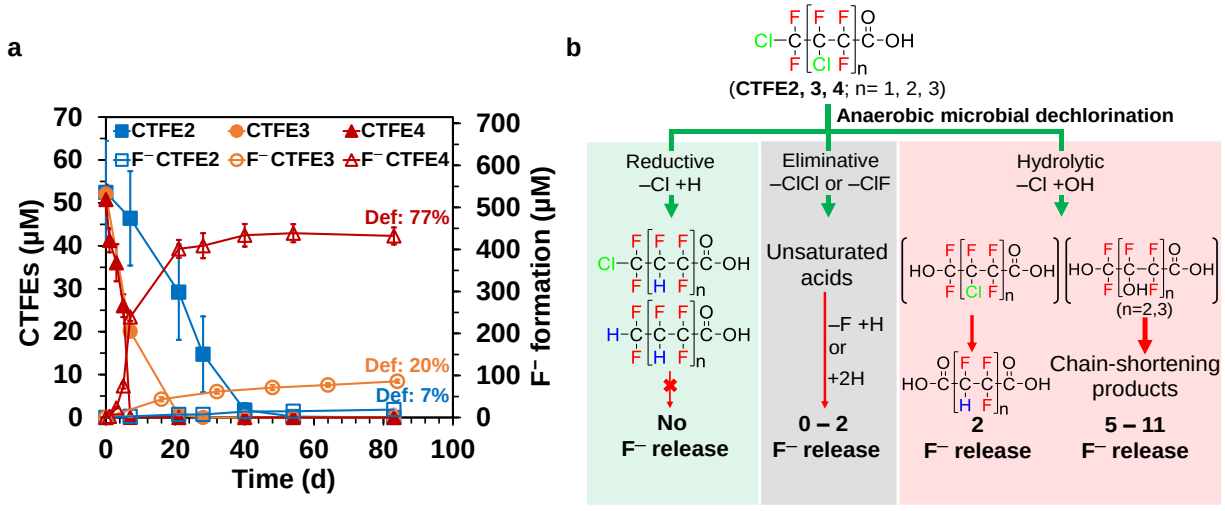

Figure 1. Biotransformation and defluorination pathways of CTFE oligomer carboxylic acids by the anaerobic microbial community. **a**, Parent compound decay and F^- formation over 84 days. Data are presented as mean values. Error bars represent the s.d. from *n* = 3 replicates. **b**, The proposed general biotransformation pathways. Green arrows represent dechlorinating reactions. Red arrows represent defluorinating reactions. The thicknesses of the red arrows represent the number of F^- release. The green-shaded panel represents the non-defluorinating pathway via reductive dechlorination (–Cl+H). The grey-shaded panel represents the defluorinating pathway via eliminative dechlorination (–ClCl or –ClF). The pink-shaded panel represents the defluorinating pathway via hydrolytic dechlorination (–Cl+OH). Note: Aerobic biotransformation or abiotic transformation was not observed, except for the slight fluoride

release from **CTFE4** in the heat-inactivated sludge control, perhaps due to some remaining biological activities, see **Figure S1** and **S2j – l**.

The hydrolytic dechlorination introduced unstable fluoroalcohol moieties, where spontaneous HF elimination would occur. For hydrolytic dechlorination at the terminal position, the formed acyl fluoride structure could be further hydrolyzed, resulting in a diacid, such as TP170 for the CTFE dimer acid (**CTFE2**) (**Figure 2b**). Two F were cleaved per molecule of TP170 formed from this defluorinating pathway. The theoretical F^- release (15.8 μM) corresponding to the 7.9 μM TP170 formed on day 192 (**Figure 2a**) was less than the actual total F^- release (26 μM) from **CTFE2**, probably due to non-detected defluorination intermediates, such as the chlorotrifluorosuccinic acid as indicated in **Figure 2b**. Assuming two F^- would be released per parent compound molecule via the defluorinating pathways, the actual 26 μM total F^- release would correspond to 13 μM of the initial 52 μM **CTFE2** being defluorinated (**Figure 2a**). Thus, the remaining majority of **CTFE2** (39 μM, 75%) underwent the non-defluorinating pathways, i.e., reductive and eliminative dechlorination (**Figure 2b**), forming more recalcitrant TPs, which exhibited slower (TP210 and TP174) or no biotransformation/defluorination (TP176) (**Figure 2a**).

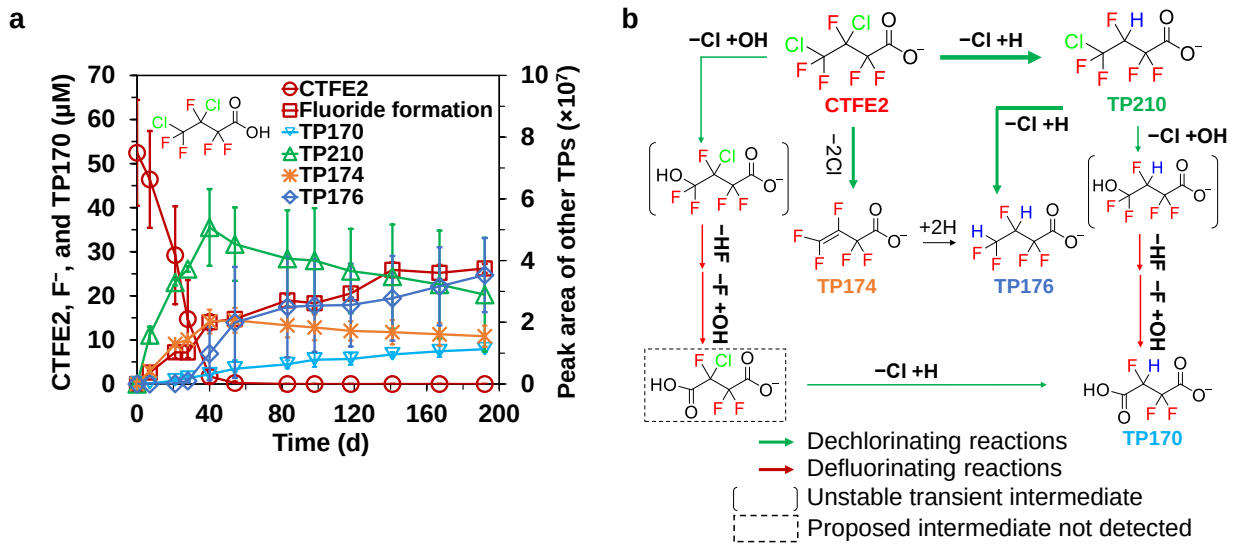

79

80 **Figure 2**. Biotransformation and defluorination pathways of **CTFE2** by the anaerobic microbial
81 community. **a**, The decay of **CTFE2** and the formation of fluoride and TPs. TP170 was
82 quantified using the reference standard and shown on the left y-axis, while the other TPs were
83 represented as peak areas on the right y-axis. Data are presented as mean values. Error bars
84 represent the s.d. from n = 3 replicates. **b**, Proposed biotransformation pathways. Green arrows
85 indicate dechlorinating reactions. Red arrows indicate defluorinating reactions. Arrow
86 thicknesses suggest the relative proportion of **CTFE2** undergoing different pathways. –Cl+H:
87 reductive dechlorination. –2Cl: eliminative dechlorination. –Cl+OH: hydrolytic dechlorination. –
88 HF: eliminative defluorination. –F+OH: hydrolytic defluorination. In brackets are unstable
89 transient intermediates, and in dashed boxes are proposed TPs not detected by LC-HRMS. See
90 **Figure S3a – d** for the LC-HRMS/MS detection of the four identified TPs.

91

92 With more CTFE monomers in the tri- and tetramer acids (**CTFE3** and **CTFE4**), the
93 biotransformation became faster. All three types of dechlorination still occurred as indicated
94 from the detected TPs, with the anaerobic hydrolytic dechlorination plus spontaneous

defluorination pathway more favored as more diacid TPs were formed (**Figure 3**). The theoretical BDE calculation (Supplemental Methods) suggested that the BDE of C–Cl bonds in **CTFE3** and **CTFE4** became lower than in **CTFE2** (**Figure S4a**), especially the middle-position ones. The C–Cl bonds with lower BDE in **CTFE3** and **CTFE4** could be more reactive in the anaerobic microbial system, particularly for the hydrolytic dechlorination, thus leading to faster biotransformation and higher defluorination.

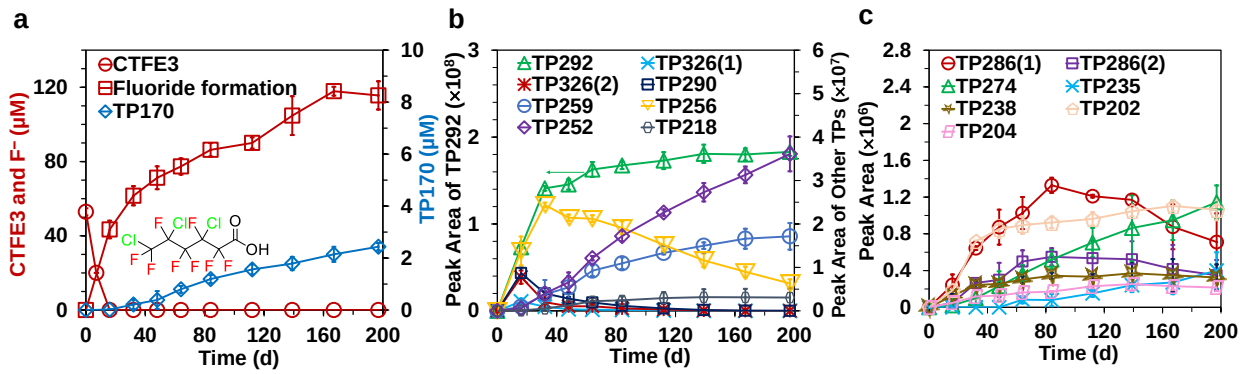

Figure 3. Biotransformation and defluorination of **CTFE3** by the anaerobic microbial community. **a**, **CTFE** decay. **b**, fluoride formation. **c**, TP formation. TP170 was quantified using the reference standard and shown in **a**, and the other TPs were shown as peak areas in **b** and **c** with different y-axis scales. Data are presented as mean values. Error bars represent the s.d. from *n* = 3 replicates.

Besides the diacid TPs with the same chain length, shorter-chain diacids were also formed from the hydrolytic dechlorination pathway, including C_4 and C_5 diacids for **CTFE3** and C_3, C_4, and C_7 diacids for **CTFE4** (**Figure 3b-c** and **Figure 4a**). The longer chain with additional Cl-substitutions in **CTFE3** and **CTFE4** likely allowed the hydrolytic dechlorination to occur at multiple Cl-substitutions in the middle of the structure simultaneously or in series. It could form fluoro keto acids ($ROC(CH_2)nCOOH$, n = 0, 1, 2), as one fluoro keto acid was

detected as a transient intermediate of **CTFE4** (TP404 in **Figure S5e** and **g**). The fluoro keto acids, if formed, would be unstable and undergo chain-shortening reactions forming the detected shorter-chain acids or diacids (**Reaction 5** in **Figure 4a**). The α-keto diacids were decarboxylated, forming one-carbon shortening TPs (i.e., TP202 and TP370 for **CTFE3** and **CTFE4**, respectively, **Figure 4a**). The C_7 diacid TP370 was one major intermediate of **CTFE4** (**Figure S5b** and **g**) and got further transformed, likely via hydrolytic dechlorination at either of the two Cl-substitutions forming C_7 β-keto fluoro diacids. C_6 and C_8 β-keto fluoro diacid intermediates were also proposed from **CTFE3** and **CTFE4**, respectively (**Figure 4a**). Those structures are unstable and subject to hydrolysis. Microbial decomposition of β-keto acids forming acetate and (n-2) acid has been reported[32]. However, difluoroacetate (DFA) was not detected, indicating that DFA was not formed from the chain-shortening reaction because DFA is recalcitrant to anaerobic defluorination (**Figure S6**) and would be accumulated and detected if formed. Two alternative scenarios were proposed: a carbene ($:CF_2COO^-$) was formed during the C–C cleavage followed by the formation of CO with F^- release, similar to the transformation of $CFCl_3$ in an anaerobic iron porphyrin/cysteine system[33], or a hydroxyl group was attached to the leaving group followed by spontaneous defluorination. The C_5 and C_6 diacids from deacetylation of the C_7 and C_8 β-keto fluoro diacids were not detected, indicating further transformation likely via hydrolytic dechlorination at the remaining Cl-substitutions forming C_5 and C_6 β-keto diacid intermediates (**Figure 4a**). The C_5 β-keto diacid could then be cleaved at the two symmetric positions leading to complete defluorination or at one position forming the stable difluoromalonic acid (TP138, structure confirmed in **Figure S5h**), a unique TP to **CTFE4**. The C_6 β-keto diacid may form a C_4 diacid, chlorotrifluorosuccinic acid (TP204), which was also the deacetylation product from **CTFE3** (**Figure 4a**). Chlorotrifluorosuccinic acid (TP204) was very

slowly biotransformed corresponding to the formation of trifluorosuccinic acid (TP170, structure confirmed in **Figure S3d**) via reductive dechlorination (**Figure 3a** and **Figure 4a**). This suggests that hydrolytic dechlorination became more difficult for C–Cl bonds in C_3 and C_4 fluoro diacids.

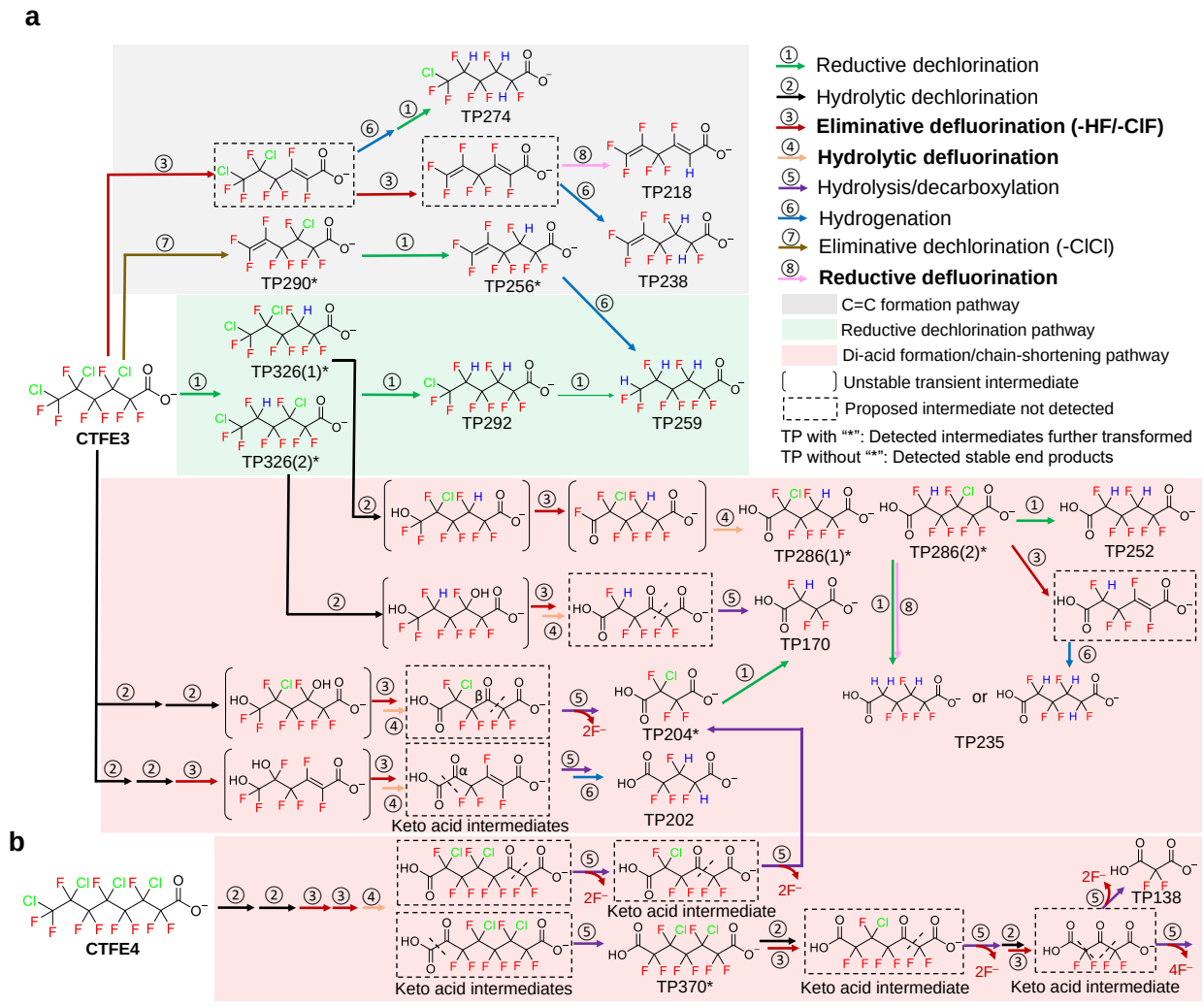

Figure 4. Proposed biotransformation pathways of **CTFE3** and **CTFE4**. **a**, proposed pathways for **CTFE3**. **b**, the proposed key defluorination pathways via hydrolytic dechlorination and chain-shortening reactions for **CTFE4**. See **Figure S5a – f** for **CTFE4** TP formation curves, **Figure S3e – p** and **Figure S5G** for the LC-HRMS/MS detection of the identified TPs of **CTFE3** and **CTFE4**, respectively.

Among the above-proposed pathways of **CTFE3** and **CTFE4**, we identified the major ones leading to the defluorination. For the quantifiable less fluorinated TPs, trifluorosuccinic acid (TP170) and difluoromalonic acid (TP138) accounted for less than 10% (1.5 – 3 μM formation, each) of the added parent compound, indicating that they are not the major end products, and their formation pathways were not major. Instead, for **CTFE3**, the formation of C_6 diacids (e.g., TP252) with 2 F^- release via the hydrolytic dechlorination pathway was more likely the major defluorination route. The deeper defluorination (3 – 5 F^- release) from chain-shortening pathways and the less defluorination (0 – 1 F^- release) from reductive and eliminative dechlorination pathways averaged out to the 27% observed defluorination degree of **CTFE3** (ca. 2 out of 8 F released per added molecule) on the last day of incubation (Day 197). Similarly, according to the 77% total defluorination of **CTFE4** after ~ 200 days, an average of 8 – 9 out of 11 F should be released per added **CTFE4** if all underwent defluorination. Since **CTFE4** partially underwent reductive and eliminative dechlorination pathways with no or much lower F^- release, we reasonably expected that a substantial portion of **CTFE4** underwent complete defluorination pathways and proposed one via the formation of a C_7 diacid (TP370) as shown in **Figure 4a**.

Dechlorination-enhanced defluorination of other PFCAs

Biotransformation activities were also significantly stimulated for other environmentally relevant Cl-PFCAs, such as the Cl-terminal and ultra-short-chain structures, in comparison to the H-substituted counterparts that exhibited no or very little biotransformation (**Figure 5a-c**, **6a-b**, **Figure S6**, **S7**, and **S8a-b**). The enhanced biodegradability was attributed to similar biodechlorination pathways as the CTFE oligomer acids underwent. In contrast to the

polychlorinated structures (i.e., CTFE oligomer acids and dichlorofluoro C_2-C_3 acids), which showed complete and fast biotransformation and defluorination (**Figure 1a** and **6a-b**), the biotransformation of monochlorinated structures (i.e., the Cl-terminal PFCAs and monochloro-perfluoro- C_2-C_3 acids) was much slower (**Table S3**). The biotransformation was incomplete after more than 160 days for the C_5 – C_9 Cl-terminal PFCAs (**Figure 5a – c**), and the C_2 – C_3 ones did not show any biotransformation (**Figure S6**). This is in line with the much higher BDE of the terminal C–Cl bond in those structures (**Figure S4b-c**).

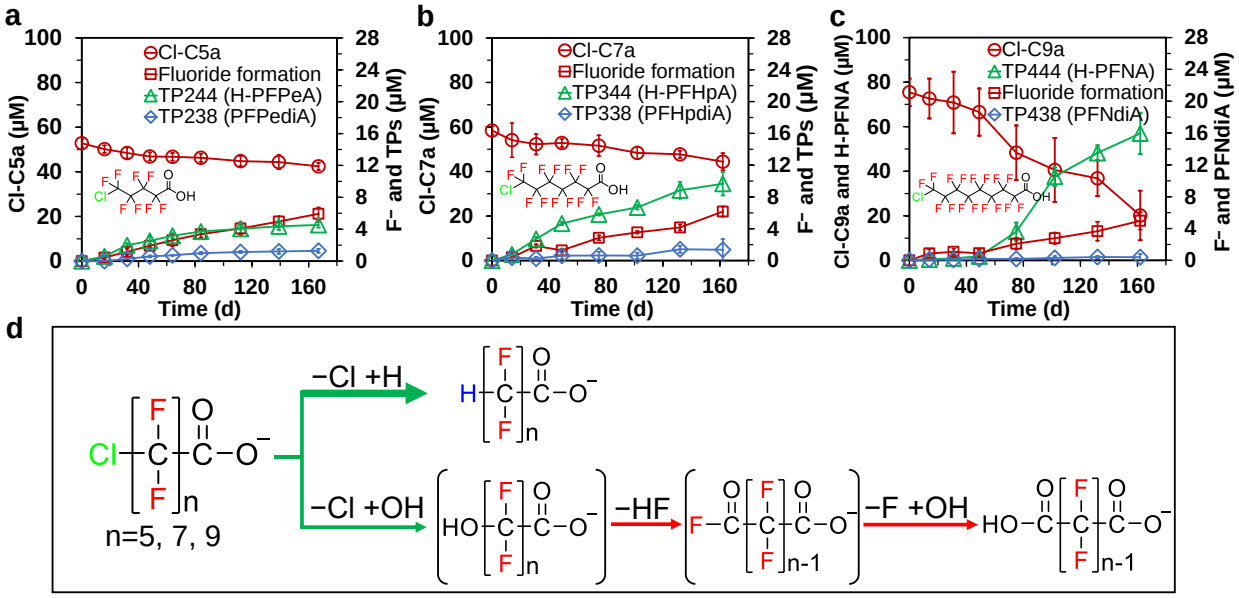

Figure 5. Biotransformation of terminal-Cl PFCAs by the anaerobic microbial community. **a-c**, Parent compound decay, F^- release, and TP formation of **Cl-C5a**, **Cl-C7a**, and **Cl-C9a**, respectively. Data are presented as mean values. Error bars represent the s.d. from $n = 3$ replicates. **d**, the proposed biotransformation pathways in common. Red arrows: defluorinating reactions. Green arrows: dechlorinating reactions. In brackets: unstable transient TPs. No aerobic or abiotic transformation or adsorption was observed, as shown in **Figure S1** and **Figure. S2g – i**. See **Figure S9** for the LC-HRMS/MS detection of the identified TPs.

All three biotransformed Cl-terminal PFCAs (n=5, 7, and 9) shared two common biotransformation pathways, the major non-defluorinating reductive dechlorination pathway and the minor defluorinating hydrolytic dechlorination pathway, the same as for the CTFE oligomer acids (**Figure 5d**). The reductive dechlorination of the parent compound was enhanced as the chain length increased (**Figure 5a – c**). More than half of **Cl-C9a** was reductively dechlorinated, while the C_5 and C_7 structures only exhibited less than 25% removal. Reductive dechlorination has been reported as the major biotransformation pathway for other Cl-terminal PFAS structures, such as 6:2 Cl-PFESA and F-53B, which were not defluorinated[29-31]. It is worth noting that significant active biosorption (~60%) was observed to **Cl-9a** (n = 9), although the tested structures with a chain length $n \leq 8$ showed less than 5% adsorption to biomass. **Cl-9a** was only taken up by actively growing biomass (**Figure S10**) but not the heat-inactivated biomass (**Figure S2i**). In comparison, the active biosorption of its two TPs (H-PFNA and PFNdiA) was much less (10 – 13%) (**Figure S10**), suggesting that the biotransformation of less mobile PFAS might result in TPs with higher mobility, thus being more easily transported into the aqueous environment.

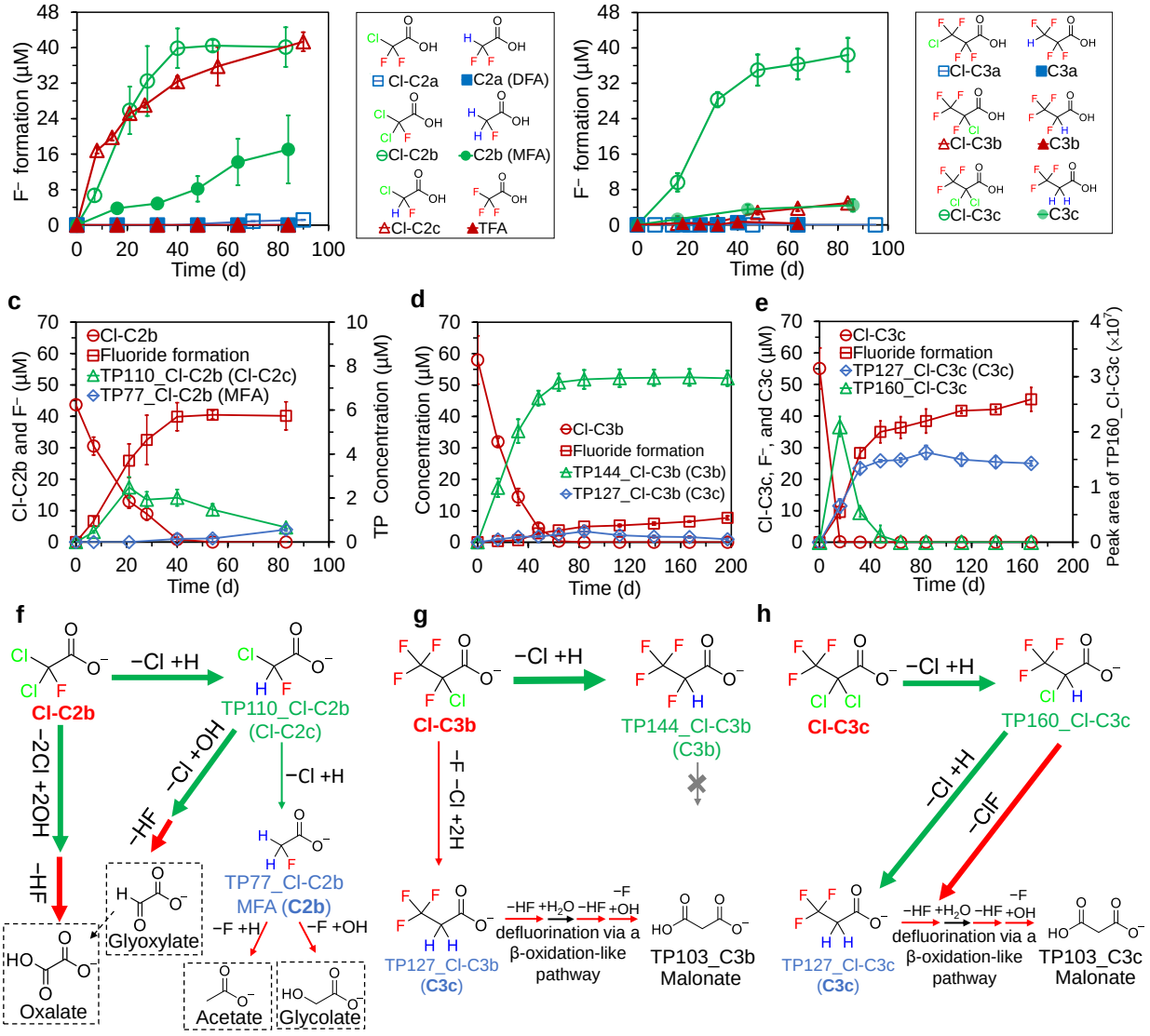

201

202 **Figure 6.** Biotransformation of C_2 and C_3 Cl-FCAs and the H-substituted counterparts by the

203 anaerobic microbial community. **a – b**, defluorination for the C2 and C3 compounds,

204 respectively. The initial concentration of parent compounds was 50 μM. Except for **Cl-C2c** that

205 showed abiotic and aerobic defluorination, all other compounds were not abiotically or

206 aerobically transformed as shown in **Figure S1** and **Figure S2a – f**. **c – e**, Parent compound

207 removal, F^- release, TP formation of **Cl-C2b**, **Cl-C3b**, and **Cl-C3c**, respectively. **f – h**, The

208 proposed biotransformation pathways of **Cl-C2b**, **Cl-C3b**, and **Cl-C3c**, respectively. Note: There

209 was no F^- formation for the three structures in the abiotic and heat-inactivated sludge controls,

except for **Cl-C3c** that exhibited non-defluorinating abiotic transformation, **Figure S2b, e, and f**; Red arrows: Defluorinating reactions. Green arrows: Dechlorinating reactions. In dashed boxes: Proposed TPs whose formation was difficult to determine due to the presence of other formation routes and further utilization during anaerobic growth. Two possible pathways for MFA are presented, i.e., hydrolytic defluorination (–F +OH)[46] and reductive defluorination (–F +H)[47]. The "β-oxidation-like pathway" was the same as reported in a previous study[34]. See **Figure S11** for the LC-HRMS/MS detection of the identified TPs. In **a – e**, data are presented as mean values. Error bars represent the s.d. from $n = 3$ replicates.

Compared to **Cl-C3a** with the terminal Cl-substitution (ω-position) that did not exhibit any biotransformation, **Cl-C3b** (2-chloro-3,3,3-trifluoropropanoic acid) with the α-Cl-substitution showed much faster and complete biotransformation (**Figure 6d**) but without defluorination (**Figure 6b**). It was reductively dechlorinated, forming the stable TP144, 2,3,3,3-tetrafluoropropanoic acid (**C3b**) (**Figure 6g**). This agrees with the lower BDE of the α-C–Cl bond in **Cl-C3b** than the ω-C–Cl bond in **Cl-C3a** (**Figure S4c**) and again suggests that C–Cl bonds closer to the carboxyl group are more reactive.

The reductive dechlorination product (TP144, **C3b**) recovered 90% of the added **Cl-C3b**, and the 10% gap (~ 6 μM) was filled up by the formation of 3,3,3-trifluoropropionate (**C3c**, TP127) (**Figure 6d**). **C3c** was the reductive dehalogenation (i.e., Cl→H and F→H exchange) product of **Cl-C3b**. Since the Cl→H product **C3b** was not further biotransformed, the F→H exchange more likely co-occurred with the reductive dechlorination. The formation of **C3c** resulted in an equal amount of F^- release (**Figures 6d** and **g**). **C3c** can be very slowly defluorinated anaerobically (**Figure 6b**), leading to slightly further F^- release after the depletion

of **Cl-C3b** (**Figure 6d**). The anaerobic defluorination of **C3c** was via the same β-oxidation-like pathway as its aerobic defluorination[34]. This was supported by the increase in malonate, the end product of this pathway (**Figure S7a**). The reductive dechlorination of 2,2-dichloro-3,3,3-trifluoropropanoic acid (**Cl-C3c**) also formed **C3c**, but the slow defluorination of **C3c** could not contribute to the rapid F^- release from **Cl-C3c** within 40 days (**Figure 6e** and **h**). Instead, the primary reductive dechlorination product TP160 seemed to partially undergo eliminative dehalogenation (–ClF) (**Figure 6h**), leading to a 1:1 release of F^-. The –ClF product was not detected as it was an intermediate of the **C3c** biodefluorination pathway and might be further transformed. This pathway led to the slower F^- release after the depletion of TP160 (**Figure 6e** and **h**).

Hydrolytic dechlorination likely occurred to the two C_2 acids (i.e., 2,2-dichloro-2-fluoroacetate (**Cl-C2b**) and its primary reductive dechlorination product 2-chloro-2-fluoroacetate (**Cl-C2c**)), which triggered the nearly complete defluorination (**Figure 6a**, **c**, and **7f**). The detected reductive dechlorination product TP77 (MFA) of **Cl-C2b** and **Cl-C2c** was at a low level, and its defluorination was slow (**Figure 6a** and **Figure S7**). Thus, the fast and complete defluorination should be triggered by the hydrolytic dechlorination of **Cl-C2b** and **Cl-C2c**. Di- and mono-chloroacetate were converted to glyoxylate by a haloacid dehalogenase in an anaerobic bacterium "*Candidatus* Dichloromethanomonas elyunquensis" strain RM via hydrolytic dechlorination[35]. Thus, it is possible that the structurally similar **Cl-C2b** and **Cl-C2c** with one C–H replaced by C–F could also undergo hydrolytic dechlorination in an anaerobic microbial community, leading to spontaneous cleavage of the C–F bond.

Microorganisms responsible for the defluorination of CTFE4

Till now, we demonstrated substantial defluorination triggered by hydrolytic dechlorination of various Cl-PFCAs. We further focused on **CTFE4** that exhibited the highest defluorination and tried to enrich the responsible microorganisms. However, during the enrichment process, the defluorination rate of **CTFE4** slowed down after four times subculturing, i.e., transferring 5% (v/v) of the previous culture into the same basal medium amended with 123 mM methanol and 50 μM **CTFE4** (**Figure 7a**). It suggested that the dehalogenation of **CTFE4** did not support or benefit the sustainable growth of the responsible microorganisms, rendering diluted biomass and decreasing defluorination activity. Since **CTFE4** dehalogenation did not lead to an outgrowth of the responsible microorganisms, the cultivation-independent metagenomic analysis would not provide clear clues of the responsible ones, as the abundant species would be most likely those grown on methanol fermentation without **CTFE4** dehalogenation.

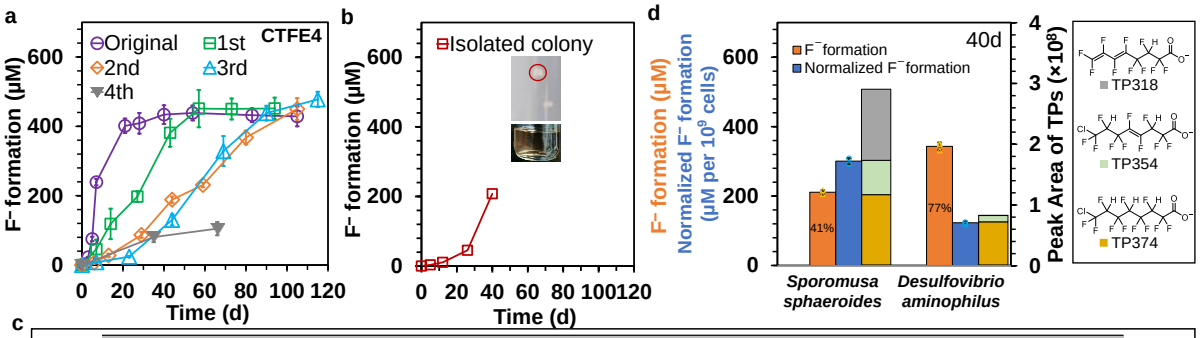

c

Bin-genome	Closest genome	Similarity (coverage) (%)	Relative abundance (%)	RDH	HAD	HAD family hydrolases	Dissimilatory sulfate reduction pathway
Bin 1	*Sporomusa sphaeroides*	97.3 (81)	35.8	0	0	1	–
Bin 2	*Desulfovibrio aminophilus*	92.0 (81)	49.0	0	0	1	+

Figure 7. **CTFE4** defluorination in subcultures of the anaerobic communities, the isolated colony, and the pure cultures. **a**, defluorination of 50 μM **CTFE4** in subcultures. Data are presented as mean values. Error bars represent the s.d. from $n = 3$ replicates, except for the 4th subculture, the error bars of which represent the s.d. from $n = 2$ replicates. **b**, Defluorination of 50 μM **CTFE4** in the colony isolated from the 3rd subculture. **c**, Information of the two major

genomes reconstructed from the metagenome of the isolated colony, RDH: reductive dehalogenase, HAD: 2-haloacid dehalogenases, HAD family hydrolases: including a variety of hydrolases, including 2-haloacid dehalogenases. **d**. total fluoride formation, cell-normalized fluoride formation, and the major stable TPs of **CTFE4** (50 μM) in *S. sphaeroides* and *D. aminophilus* after 40 days. Data are presented as mean values. Error bars represent the s.d. from $n = 2$ replicates for *S. sphaeroides* and $n = 3$ replicates for *D. aminophilus*. The dot plots represent raw data of total fluoride formation (yellow triangles) and the cell-normalized fluoride formation (blue circles). The average total defluorination percentage is indicated in the first column. A representative isomer structure of TP354 and TP318 is shown. See **Figure S5g** for all possible isomer structures.

Alternatively, we used the isolation approach to identify responsible microbes. From the 3rd subculture, we isolated and screened one colony that exhibited a similar **CTFE4** defluorination activity as the 3rd subculture in the same medium after 40 days (**Figure 7b**). It was a highly enriched culture consisting of two dominant bingenomes, which are closest to *Sporomusa sphaeroides* and *Desulfovibrio aminophilus* (**Figure 7c** and **Table S4**). We then obtained the two pure cultures, i.e., *S. sphaeroides* (DSM 2875) and *D. aminophilus* (DSM 12254), which exhibited complete removal of **CTFE4** after 14 and 21 days, respectively (**Figure S12**). The total defluorination was about two-fold higher in *D. aminophilus* (77%) than in *S. sphaeroides* (41%) (**Figure 7d**). The faster removal and higher defluorination of **CTFE4** in *D. aminophilus* could be attributed to its higher growth than *S. sphaeroides*, and the latter had a higher (2.4×) defluorination capacity per cell. Additionally, *S. sphaeroides* converted more **CTFE4** into the less defluorinated stable products via reductive and eliminative dechlorination

(**Figure 7d**), and this could also render the lower total defluorination than *D. aminophilus*. Given the phylogenetically insignificant similarity of the two identified genomes to the two tested pure strains, as well as the phylogenetic divergence between the two genomes, **CTFE4-**degrading microorganisms might be less specific across the same genus and commonly occurring in anaerobic environments. Knowing the characteristics of the defluorinating microorganisms could help enhance the defluorination in a microbial community. Given that the *Desulfovibrio*-like bingenome possesses dissimilatory sulfate reduction pathways (**Figure 8c**)[36], by providing sulfate to the 4th subculture of the **CTFE4**-defluorinating microcosm with declined defluorination activity (**Figure 7a**), we selectively stimulated the growth of the defluorinating sulfate reducers in the community, thus significantly boosted the defluorination of **CTFE4** (**Figure S13**). Neither of the two bingenomes has genes annotated as reductive dehalogenases or 2-haloacid dehalogenases (HAD) (**Figure 7c**). Only one HAD family hydrolase gene with unclear specific function was annotated in the two bingenomes with 40% amino acid similarity. Whether the HAD family protein could catalyze the hydrolytic dechlorination of **CTFE4** remains unclear and warrants future investigation.

Implications for the PFAS research field

PTFE and PCTFE are the two widely used fluoropolymers. Compared to PTFE, PCTFE with one F substituted by Cl in the CTFE monomer would become more biodegradable and less persistent in the environment once transformed into CTFE oligomer carboxylic acids via thermal decomposition[9-11] or biological oxidative metabolism[12,13]. Our findings also indicate that longer-chain CTFE oligomer acids may have an even shorter half-life and undergo much deeper defluorination in anaerobic environments, where the identified responsible microorganisms

(*Desulfovibrio* and *Sporomusa* species) could be commonly distributed[37-40]. It is worth noting that despite the enhanced bioavailability of the Cl-substituted structures, only specific types of dechlorination, i.e., hydrolytic and eliminative dechlorination, could trigger the defluorination of CTFE oligomer acids. The importance of previously underestimated non-respiratory hydrolytic dechlorination genes in chlorinated natural organic matter cycling was recently highlighted, given their high detection frequencies in the environment[37]. Here, we further demonstrate another critical role they may play in the deep defluorination of chlorinated PFAS.

The higher biodegradation potential of chlorinated PFAS could provide critical guidance for the design of alternative PFAS that are more readily biodegradable and meanwhile have similar functionality and no increase in toxicity. It is commonly thought that the increase in the number of Cl substitutions could render higher toxicity. This seems not to be the case regarding the microbial toxicity of chlorinated PFAS. The mono- and poly Cl-PFCAs (C_4-C_9) investigated in this study showed less inhibition than PFCAs with the same chain length on the luminescence of *Vibrio fischeri* (**Figure S14**), the standard toxicity measurement[41]. In contrast, the H-terminal PFCAs, one major biotransformation product of Cl-terminal PFCAs, exhibited a higher inhibitory effect on the luminescence than the parent compound. One should note that the luminescent bacteria test only indicates acute microbial toxicity. Toxicity tests using higher organisms are needed to obtain a comprehensive and systematic evaluation of the ecotoxicity of chlorinated PFAS.

People may have another concern that although Cl-substitutions enhanced biodegradability, complete defluorination was still not achieved due to the non-defluorinating biotransformation pathways, such as the reductive dechlorination pathway. The incompletely defluorinated products might be more mobile in the aquatic environment with higher toxicities to

342 the ecosystem. Nonetheless, since many of them contain C–H bonds at saturated and unsaturated
343 carbons, they are prone to be biodegraded aerobically, as indicated in our previous studies[20,34].
344 We collected the spent medium of cultures after reaching the maximum anaerobic defluorination
345 (~80%) of the CTFE tetramer acid and further treated it aerobically using the activated sludge
346 community collected from the same WWTP. An additional 12% defluorination was achieved
347 after 9 days (**Figure S15**). Therefore, a sequential anaerobic-aerobic bioreactor could be adapted
348 from the commonly employed anaerobic-aerobic configurations for municipal or industrial
349 wastewater treatment by increasing the anaerobic sludge retention time to cost-effectively treat
350 wastewater containing CTFE tetramer acid. Nearly complete destruction of the tetramer acid that
351 enters aquatic environments may also be expected at an anaerobic and aerobic interface in
352 nature.

353 The identified novel biotransformation pathways of Cl-PFCA also provide important
354 insights into PFAS source-tracking, environmental monitoring, and risk assessment. Besides the
355 reported H-PFCAs from reductive dechlorination, two new groups of TPs, i.e., PFdiCAs and
356 unsaturated FCAs, were experimentally demonstrated from the anaerobic biotransformation of
357 various Cl-PFCAs. Thus, Cl-PFAS could be a critical source of all the above three classes of
358 emerging PFAS detected in different environments[25,42]. This is supported by the observations in
359 recent studies[25,43], which revealed correlations between the detection of H-substituted,
360 unsaturated, and diacid products and the occurrence of Cl-PFAS in impacted wastewater and
361 soils. Thus, closer and more accurate PFAS monitoring and toxicity studies could also be done
362 on the non- and slowly biotransformed Cl-PFAS, as well as the stable end products (e.g., H-
363 PFCAs, PFdiCAs, and unsaturated PFCAs) given their persistence in the aquatic environment.

The discovery of the new capabilities of commonly occurring anaerobic microorganisms in transforming and defluorinating industrially critical Cl-PFAS not only advances the current fundamental knowledge of microbial dehalogenation but also provides significant insights into a more accurate assessment of the environmental fate and ecotoxicity of Cl-PFAS, the design of readily biodegradable and less toxic alternative PFAS, and the development of cost-effective bioremediation strategies.

Methods

Chemicals. Twelve chlorine-substituted polyfluorinated carboxylic acids (Cl-PFCAs, see **Table S1** for detailed information) investigated in this study were purchased from SynQuest Laboratories, Inc., Matrix Scientific, and Manchester Organics, Ltd. Stock solutions (~10 mM) of individual Cl-PFCAs and other reference compounds of plausible transformation products (**Table S2**) were prepared in methanol (HPLC grade). All the stock solutions were stored at –20 °C.

Anaerobic Biotransformation. The activated sludge community freshly taken from a local municipal WWTP was used. To avoid the carryover of dissolved oxygen, settled activated sludge (6700 – 6800 mg suspended solids/L) was inoculated (10%, v/v) into a 160-mL sealed serum bottle containing 90 mL autoclaved basal medium with vitamins including 100 μg/L B_{12}, as previously described[44], and a 60-mL headspace of Ar/CO_2 (75:25, v/v). Methanol (~123 mM), as an electron donor, was added into the culture and re-added bi-weekly. The selected PFAS (~50 μM) was spiked into the culture. The culture pH was buffered at 7.4 ± 0.1. Biomass-free abiotic and heat-inactivated biomass controls were set up in the same way, using autoclaved sludge filtrate (0.22 μm) and autoclaved sludge instead of the activated sludge as the inoculum,

387 respectively. In both abiotic and heat-inactivated biomass controls, sodium azide was added (~
388 0.2 g/L) to further inhibit microbial activities over the entire incubation. All cultures were
389 incubated in the dark at 34 °C without shaking. The biotransformation groups, abiotic, and heat-
390 inactivated controls were performed in triplicates. One sludge-only control bottle was also
391 included to account for the sludge matrix, which was subtracted in the transformation product
392 (TP) analysis.

393 Samples (2 mL) were taken periodically and then centrifuged at 16,000× g at 4 °C for 35
394 min. The supernatant was collected for the measurement of fluoride, the parent compound, and
395 TPs by the following instrumental analyses. Cell pellets were collected and extracted using 1 mL
396 of methanol with 0.1% NH_4OH. The ^{13}C-labeled PFOA surrogate was spiked to account for the
397 extraction recovery. Samples were vortexed and ultrasonicated for 30 min, then centrifuged at
398 16,000× g at 4 °C for 35 min. Parent compounds and TPs in the extracted samples were analyzed
399 to account for biomass adsorption. Except for **Cl-C9a**, which exhibited significant biological
400 adsorption, all tested Cl-PFCAs showed less than 5% adsorption in biomass. Thus, extracellular
401 concentrations of parent compounds and TPs were used to interpret biotransformation pathways,
402 except for **Cl-C9a** and its TPs, for which the total concentrations (extracellular and biomass-
403 associated) were used. The half-lives of parent compounds were determined using the first-order
404 reaction kinetics assumption (see the details in the Supplemental Methods).

405 **Aerobic Biotransformation.** The aerobic biotransformation experiments were conducted using
406 a similar setup as a previous study[34]. Fifty mL of fresh activated sludge (~4400 mg/L as TSS)
407 was inoculated into batch reactors (150 mL, loosely capped) spiked with ~50 µM of Cl-PFCAs
408 and incubated with shaking (150 rpm) at room temperature for 5 days. The dissolved oxygen
409 level in the reactors was measured and stayed at 4 – 5 mg/L over the time course. Heat-

410 inactivated controls were prepared using autoclaved (121 °C, 40 min) sludge and autoclaved
411 sludge filtrate (0.22 μm filter). A sludge-only control was also performed to obtain the F^-
412 concentration in the sludge matrix, which did not show significant change throughout the
413 incubation period.
414 **Fluoride Measurement**. Fluoride (F^-) was measured by an HQ30D Portable Multi Meter
415 (HACH) connected with an ion-selective electrode (ISE, HACH) with the limit of quantification
416 (LOQ) of 0.01 mg/L (c.a. 0.5 μM). First, 0.1 g of fluoride ionic strength adjustor powder
417 (HACH) was dissolved into two milliliters of sample. Then, calibration was conducted using
418 three standard fluoride solutions (0.5 mg/L, 1 mg/L, and 2 mg/L, HACH). It was done every time
419 before the sample measurement. Samples were diluted into the calibration range, as needed,
420 before measurement. The fluoride measurement was cross-validated by ion chromatography (IC)
421 (See Supplemental Methods). F^- formation was calculated by subtracting the F^- concentration at
422 t_0 from that at time t. Defluorination degree was determined by the following equation.

423 $$\text{Defluorination degree (\%)} = \frac{F^- \text{ formation } (\mu M)}{\text{Removed conc.(uM)} \times \#\text{ of F in one molecule}} \times 100\%$$

424 **Ultra-High-Performance Liquid Chromatography Coupled to High-Resolution Mass**
425 **Spectrometry (UHPLC-HRMS) Analysis**. All organofluorines were analyzed by a UHPLC-
426 HRMS/MS, Q Exactive Plus, Thermo Fisher Scientific). For the UHPLC, the mobile phase
427 consisted of (A) 10 mM ammonium acetate in Milli-Q water and (B) 10 mM ammonium acetate
428 in HPLC-grade methanol. A two-microliter sample was loaded onto a Hypersil Gold column
429 (particle size 1.9 μm, 2.1×100 mm, Thermo Fisher Scientific) and eluted with a flow rate of 300
430 μL/min. The linear gradient was 95% A for 0 – 1 min, 95 – 5% A for 1 – 6 min, 5% A for 6 – 8
431 min, and 95% A for 8 – 10 min. For HRMS, the negative electrospray ionization (ESI–) was
432 employed for the sample ionization with the default charge of one. The mass analyzer was set up

with both a full MS scan (m/z 50-750) at a resolution of 140,000 @ m/z 200 and a data-dependent MS^2 scan (dd-MS^2) at a resolution of 17,500 @ m/z 200 with normalized collision energy (NCE) of 25.

The peak areas of all parent compounds and transformation products were obtained by TraceFinder 4.1 EFS and Freestyle 1.6 (Thermo Fisher Scientific). Mass spectrometry information, including MS^1 and MS^2, was primarily gained by Freestyle 1.6. Concentrations of the parent compound and TPs with reference standards were determined by establishing external calibration curves using matrix-match calibration standard series.

Transformation Product (TP) Identification and Biotransformation Pathway Elucidation. The suspect screening was conducted using a custom-compiled suspect list, including the possible reductive defluorination and reductive dechlorination products[19]. The non-target screening was also employed in TP analysis by using the modified "Expected and Unknown Met ID (Metabolite identification) Workflow" in Compound Discover 3.1 (Thermo Fisher Scientific). Plausible TPs were identified using the following criteria: (1) mass tolerance ($\leq$ 5 ppm); (2) proper peak shape with peak area larger than 10^5; (3) isotopic pattern score > 70; (4) significant formation trend over time (increasing or increasing followed by decreasing); (5) not detected in the abiotic, heat-inactivated or sludge-only controls; and (6) not identified as in-source fragments[19]. The structures of plausible TPs were further elucidated according to the MS^2 fragmentation profiles. For TPs with the reference compound available, the structures were confirmed by comparing the retention time (RT) and MS^1/MS^2 profiles between the TP and the reference compound. Confidence levels of TPs were determined according to the criteria set by Schymanski *et al*[45].

We proposed the most reasonable biotransformation pathways based on the three trends: (i) the removal trend of the parent compound, (ii) the formation trend of TPs with accurate formula or identified structure, and (iii) the fluoride formation trend. The three trends should be intercorrelated. For example, for biotransformation pathways including multiple levels of reactions, TPs from the primary reactions should exhibit a formation trend that first increases, then decreases, followed by the formation of secondary TPs. Generally, primary transient TPs peaked when most of the parent compound was gone, then the corresponding secondary TPs started to increase significantly, and the same applied for the next level of reactions. Stable products (or end products) were those with an increasing trend or increasing with a plateau if the precursor was depleted. The formation of fluoride should correspond to the formation of less-fluorinated TPs.

CTFE4-defluorinating subcultures. The original **CTFE4**-defluorinating anaerobic microcosm obtained from the activated sludge was subcultured (5%, v/v) into the same basal medium containing the same concentrations of methanol and **CTFE4**. After the defluorination reached the maximum level (~80%), the last subculture was further transferred (5%, v/v) into the same medium to get the subsequent subcultures.

Anaerobic Isolation. Anaerobic agar shake tubes were used to isolate and purify colonies from the **CTFE4**-defluorinating subcultures. In each 20-mL sealed glass tube, there was 10 mL sterile agar (0.3 – 0.5%, w/w) medium containing the same nutrients (i.e., mineral salts, vitamins, methanol, and **CTFE4**) as in the broth medium and an N_2 headspace. The tubes were incubated at 45 – 50°C before the inoculation. After the temperature of the agar medium slightly dropped, one agar shake tube was inoculated with 1 mL of the third subculture, then gently mixed by inverting the tube several times. One mL of mixed liquid was then transferred into a new agar

shake tube. A set of inoculated agar shake tubes with 10^{-1} – 10^{-8} dilution series were solidified and incubated at 34℃. After 14 days of incubation, individual colonies were picked up using syringe needles and inoculated into new agar shake tubes for further purification. Further purified individual colonies with different morphology were picked up and transferred into the same liquid basal medium amended with methanol (~123 mM) and **CTFE4** for the defluorination activity test. The liquid cultures from two colonies, which showed defluorination activity, were subject to metagenomic sequencing for genomic composition analysis.

Metagenomic sequencing. Cells in liquid cultures were collected by centrifugation at 18,000 g for 20 min at room temperature. Genomic DNA was extracted using DNeasy Blood and Tissue Kit (Qiagen, Redwood City, CA) according to the manufacturer's instruction and then sent to Microbial Genome Sequencing Center (Pittsburg, PA) for sequencing (Illumina NextSeq 2000, 2 × 150 bp, 680 Mbp output).

Reconstruction of bingenomes. The draft genome assembly and binning were performed on the Department of Energy Systems Biology Knowledgebase (KBase) platform (https://www.kbase.us/). The sequencing reads of each sample were trimmed and quality-filtered using Trimmomatic v 0.36 with default parameters. The clean reads were assembled into contigs by MEGAHIT v1.2.9, and the contigs were then binned using MetaBAT v1.7. The quality (i.e., completeness and contamination) of the reconstructed bingenomes was assessed using CheckM v1.0.18. Bingenomes with > 85% completeness and < 5% contamination were considered as successfully reconstructed ones and subject to the downstream analysis. The taxonomic assignment of the reconstructed bingenomes was assessed using GTDB-TK v1.3.0, and the genome annotation was generated by RASTtk v1.073. The relative abundance of each reconstructed bingenome was calculated by mapping the quality-filtered sequence reads against

the reconstructed bingenome using Bowtie2 v2.3.2. The percentage of mapped reads out of the total reads was regarded as the relative abundance of the reconstructed bingenome.

CTFE4 defluorination by pure cultures. The two pure cultures, i.e., *Sporomusa spaeroides* and *Desulfovibrio aminophilus*, were obtained from DSMZ-German Collection of Microorganisms and Cell Cultures GmbH under the DSM numbers 2875 and 12254, respectively. Both cultures were maintained in the same basal medium used for the anaerobic biotransformation by the sludge community, as described above, with the addition of 20 mM lactate as the electron donor. For the sulfate-reducing *D. aminophilus*, sulfate (2 mM) was also added. For the **CTFE4** defluorination test, each culture was inoculated (10%, v/v) into 50 mL fresh medium containing the same growth substrates and 50 μM **CTFE4**. After ~40 days, cells were collected by centrifugation at 18,000 × g for 20 min at room temperature for DNA extraction to determine the cell density (See Supplemental Methods). The supernatant was subject to F^- and **CTFE4** analysis.

Data Availability

The metagenomic sequencing dataset were deposited to Sequence Read Archive under the accession number PRJNA838587.

The draft genomes of the two dominant bacterial species in the isolated defluorinating colonies were deposited to GenBank under the accession numbers JAMHFZ000000000 and JAMHGA000000000.

All other data supporting the findings in this study are available within the paper and its Supplementary Information. Source data are provided with this paper.

Acknowledgements

This work was supported by the Strategic Environmental Research and Development Program (Project No. ER20-1541, for B.J., Y.Y., J.G., J.L., and Y.M.) and National Institute of Environmental Health Sciences (Award No. R01ES032668, for H.L., S.C., and Y.M.).

Author Contributions

Y.M. and B.J. conceived and designed the project, analyzed the data, and prepared the manuscript. B.J. conducted the anaerobic biotransformation experiments using the anaerobic microbial community and pure cultures and analyzed the LC-HRMS/MS and sequencing data. S.C. performed the aerobic biotransformation experiments and contributed to the anaerobic biotransformation setup. H.L. performed the anaerobic isolation and sample preparation for metagenomic sequencing. Y.Y. contributed to the analytical and sequencing data analysis. J.G. contributed to the calculation of the BDE. J.L. contributed to the PFAS compound selection and mechanistic discussion.

Competing Interests

The authors declare no competing interests.

References

1 Dolbier, W. R. Fluorine chemistry at the millennium. *J. Fluor. Chem.* **126**, 157-163 (2005). https://doi.org:10.1016/j.jfluchem.2004.09.033

2 Lohmann, R. *et al.* Are fluoropolymers really of low concern for human and environmental health and separate from other PFAS? *Environ. Sci. Technol.* **54**, 12820-12828 (2020). https://doi.org:10.1021/acs.est.0c03244

3 Evich, M. G. *et al.* Per- and polyfluoroalkyl substances in the environment. *Science* **375**, eabg9065 (2022). https://doi.org:10.1126/science.abg9065

4 Xiao, F. Emerging poly- and perfluoroalkyl substances in the aquatic environment: A review of current literature. *Water Res.* **124**, 482-495 (2017). https://doi.org:10.1016/j.watres.2017.07.024

5 Kotthoff, M. & Bucking, M. Four chemical trends will shape the next decade's directions in perfluoroalkyl and polyfluoroalkyl substances research. *Front. Chem.* **6**, 103 (2018). https://doi.org:10.3389/fchem.2018.00103

6 Dams, R. & Hintzer, K. in *Fluorinated Polymers: Volume 2: Applications* Vol. 2 1-31 (The Royal Society of Chemistry, 2017).

7 Vanbrocklin, C. Military applications of chlorotrifluoroethylene oligomer base nonflammable hydraulic fluid. *J. Fire Sci.* **11**, 232-241 (1993). https://doi.org:Doi 10.1177/073490419301100303

8 Gschweder, L., Mattie, D., Syder, C., Warer, W. & van Brocklin, C. Chlorotrifluoroethylene oligomer based nonflammable hydraulic fluid. 1 Fluid, additive, and elastomer development. *J. Synth. Lubr.* **9**, 187-203 (1992). https://doi.org:10.1002/jsl.3000090302

9 Ellis, D. A., Mabury, S. A., Martin, J. W. & Muir, D. C. Thermolysis of fluoropolymers as a potential source of halogenated organic acids in the environment. *Nature* **412**, 321-324 (2001). https://doi.org:10.1038/35085548

10 Myers, A. L., Jobst, K. J., Mabury, S. A. & Reiner, E. J. Using mass defect plots as a discovery tool to identify novel fluoropolymer thermal decomposition products. *J. Mass Spectrom.* **49**, 291-296 (2014). https://doi.org:https://doi.org/10.1002/jms.3340

11 Dias, J. *et al.* Thermal degradation behavior of ionic liquid/fluorinated polymer composites: Effect of polymer type and ionic liquid anion and cation. *Polymer*, 123995 (2021).

12 DelRaso, N. J., Auten, K. L., Higman, H. C. & Leahy, H. F. Evidence of hepatic conversion of C_6 and C_8 chlorotrifluoroethylene (CTFE) oligomers to their corresponding CTFE acids. *Toxicol. Lett.* **59**, 41-49 (1991). https://doi.org:10.1016/0378-4274(91)90053-9

13 Brashear, W. T., Greene, R. J. & Mahle, D. A. Structural determination of the carboxylic acid metabolites of polychlorotrifluoroethylene. *Xenobiotica* **22**, 499-506 (1992). https://doi.org:10.3109/00498259209053112

14 Song, X., Vestergren, R., Shi, Y., Huang, J. & Cai, Y. Emissions, transport, and fate of emerging per- and polyfluoroalkyl substances from one of the major fluoropolymer manufacturing facilities in China. *Environ. Sci. Technol.* **52**, 9694-9703 (2018). https://doi.org:10.1021/acs.est.7b06657

15 Fujiwara, M., Jodry, J. J. & Narizuka, S. Process for producing alkoxycarbonylfluoroalkanesulfonates. United States patent US20080108846A1 (2008).

16 Yin, H., Anders, M. W. & Jones, J. P. Metabolism of 1,2-dichloro-1-fluoroethane and 1-fluoro-1,2,2-trichloroethane: electronic factors govern the regioselectivity of cytochrome P450-dependent oxidation. *Chem. Res. Toxicol.* **9**, 50-57 (1996). https://doi.org:10.1021/tx950086n

17 Harris, J. W. & Anders, M. W. Metabolism of the hydrochlorofluorocarbon 1,2-dichloro-1,1-difluoroethane. *Chem. Res. Toxicol.* **4**, 180-186 (1991). https://doi.org:10.1021/tx00020a009

18 Liu, J. & Mejia Avendano, S. Microbial degradation of polyfluoroalkyl chemicals in the environment: a review. *Environ. Int.* **61**, 98-114 (2013). https://doi.org:10.1016/j.envint.2013.08.022

19 Yu, Y. *et al.* Microbial cleavage of C-F bonds in two C_6 per- and polyfluorinated compounds via reductive defluorination. *Environ. Sci. Technol.* **54**, 14393-14402 (2020). https://doi.org:10.1021/acs.est.0c04483

20 Yu, Y. *et al.* Microbial defluorination of unsaturated per- and polyfluorinated carboxylic acids under anaerobic and aerobic conditions: A structure specificity study. *Environ. Sci. Technol.* **56**, 4894-4904 (2022). https://doi.org:10.1021/acs.est.1c05509

21 Wackett, L. P. Nothing lasts forever: understanding microbial biodegradation of polyfluorinated compounds and perfluorinated alkyl substances. *Microb. Biotechnol.*, 1-20 (2021). https://doi.org:10.1111/1751-7915.13928

22 Adrian, L. & Löffler, F. E. *Organohalide-respiring bacteria*. (Springer, 2016).

23 Zhang, B. *et al.* Novel and legacy poly- and perfluoroalkyl substances (PFASs) in indoor dust from urban, industrial, and e-waste dismantling areas: The emergence of PFAS

alternatives in China. *Environ. Pollut.* **263**, 114461 (2020). https://doi.org:10.1016/j.envpol.2020.114461

24 Liu, W. *et al.* Atmospheric chlorinated polyfluorinated ether sulfonate and ionic perfluoroalkyl acids in 2006 to 2014 in Dalian, China. *Environ. Toxicol. Chem.* **36**, 2581-2586 (2017). https://doi.org:10.1002/etc.3810

25 Wang, Y. *et al.* Suspect and nontarget screening of per- and polyfluoroalkyl substances in wastewater from a fluorochemical manufacturing Park. *Environ. Sci. Technol.* **52**, 11007-11016 (2018). https://doi.org:10.1021/acs.est.8b03030

26 Liu, Y., Qian, M., Ma, X., Zhu, L. & Martin, J. W. Nontarget mass spectrometry reveals new perfluoroalkyl substances in fish from the Yangtze River and Tangxun Lake, China. *Environ. Sci. Technol.* **52**, 5830-5840 (2018). https://doi.org:10.1021/acs.est.8b00779

27 Washington, J. W. *et al.* Nontargeted mass-spectral detection of chloroperfluoropolyether carboxylates in New Jersey soils. *Science* **368**, 1103-1107 (2020). https://doi.org:10.1126/science.aba7127

28 MacInnis, J. J., Lehnherr, I., Muir, D. C. G., Quinlan, R. & De Silva, A. O. Characterization of perfluoroalkyl substances in sediment cores from High and Low Arctic lakes in Canada. *Sci. Total Environ.* **666**, 414-422 (2019). https://doi.org:10.1016/j.scitotenv.2019.02.210

29 Lin, Y., Ruan, T., Liu, A. & Jiang, G. Identification of Novel Hydrogen-Substituted Polyfluoroalkyl Ether Sulfonates in Environmental Matrices near Metal-Plating Facilities. *Environ. Sci. Technol.* **51**, 11588-11596 (2017). https://doi.org:10.1021/acs.est.7b02961

30 Yi, S., Zhu, L. & Mabury, S. A. First Report on In Vivo Pharmacokinetics and Biotransformation of Chlorinated Polyfluoroalkyl Ether Sulfonates in Rainbow Trout. *Environ. Sci. Technol.* **54**, 345-354 (2020). https://doi.org:10.1021/acs.est.9b05258

31 Yi, S., Yang, D., Zhu, L. & Mabury, S. A. Significant reductive transformation of 6:2 chlorinated polyfluorooctane ether sulfonate to form hydrogen-substituted polyfluorooctane ether sulfonate and their toxicokinetics in male Sprague-Dawley rats. *Environ. Sci. Technol.*, 10.1021/acs.est.1021c00616 (2021). https://doi.org:10.1021/acs.est.1c00616

32 Lieberman, I. & Barker, H. A. β-keto acid formation and decomposition by preparations of *Clostridium kluyveri*. *J. Bacteriol.* **68**, 329-333 (1954). https://doi.org:doi:10.1128/jb.68.3.329-333.1954

33 Buschmann, J., Angst, W. & Schwarzenbach, R. P. Iron porphyrin and cysteine mediated reduction of ten polyhalogenated methanes in homogeneous aqueous solution: Product analyses and mechanistic considerations. *Environ. Sci. Technol.* **33**, 1015-1020 (1999). https://doi.org:10.1021/es980553y

34 Che, S. *et al.* Structure-Specific Aerobic Defluorination of Short-Chain Fluorinated Carboxylic Acids by Activated Sludge Communities. *Environ. Sci. Technol. Lett.* **8**, 668-674 (2021). https://doi.org:10.1021/acs.estlett.1c00511

35 Chen, G. *et al.* Anaerobic microbial metabolism of dichloroacetate. *mBio.* **12** (2021). https://doi.org:10.1128/mBio.00537-21

36 Möller, B., Oßmer, R., Howard, B. H., Gottschalk, G. & Hippe, H. *Sporomusa*, a new genus of gram-negative anaerobic bacteria including *Sporomusa sphaeroides* spec. nov.

and *Sporomusa ovata* spec. nov. *Arch. Microbiol.* **139**, 388-396 (1984). https://doi.org:10.1007/BF00408385

37 Temme, H. R., Carlson, A. & Novak, P. J. Presence, diversity, and enrichment of respiratory reductive dehalogenase and non-respiratory hydrolytic and oxidative dehalogenase genes in terrestrial environments. *Front. Microbiol.* **10**, 1258 (2019). https://doi.org:10.3389/fmicb.2019.01258

38 Duhamel, M. & Edwards, E. A. Microbial composition of chlorinated ethene-degrading cultures dominated by Dehalococcoides. *FEMS Microbiol. Ecol.* **58**, 538-549 (2006). https://doi.org:10.1111/j.1574-6941.2006.00191.x

39 Baena, S. *et al.* Desulfovibrio aminophilus sp. nov., a Novel Amino Acid Degrading and Sulfate Reducing Bacterium from an Anaerobic Dairy Wastewater Lagoon. *Systematic and Applied Microbiology* **21**, 498-504 (1998). https://doi.org:https://doi.org/10.1016/S0723-2020(98)80061-1

40 Yang, Y., Pesaro, M., Sigler, W. & Zeyer, J. Identification of microorganisms involved in reductive dehalogenation of chlorinated ethenes in an anaerobic microbial community. *Water Res.* **39**, 3954-3966 (2005). https://doi.org:https://doi.org/10.1016/j.watres.2005.07.010

41 ISO 11348-3: 2007, *Water quality - Determination of the inhibitory effect of water samples on the light emission of Vibrio fischeri (Luminescent bacteria test) - Part 3: Method using freeze-dried bacteria*.

42 Newton, S. *et al.* Novel polyfluorinated compounds identified using high resolution mass spectrometry downstream of manufacturing facilities near Decatur, Alabama. *Environ. Sci. Technol.* **51**, 1544-1552 (2017). https://doi.org:10.1021/acs.est.6b05330

43 Evich, M. G. *et al.* Environmental Fate of Cl-PFPECAs: Predicting the Formation of PFAS Transformation Products in New Jersey Soils. *Environ. Sci. Technol.* (2022). https://doi.org:10.1021/acs.est.1c06126

44 Men, Y. *et al.* Sustainable syntrophic growth of *Dehalococcoides ethenogenes* strain 195 with *Desulfovibrio vulgaris* Hildenborough and *Methanobacterium congolense*: global transcriptomic and proteomic analyses. *ISME J.* **6**, 410-421 (2012). https://doi.org:10.1038/ismej.2011.111

45 Schymanski, E. L. *et al.* Identifying small molecules via high resolution mass spectrometry: communicating confidence. *Environ. Sci. Technol.* **48**, 2097-2098 (2014). https://doi.org:10.1021/es5002105